

Chapter 2

Lecture 6

Longitudinal stick-fixed static stability and control – 3

Topics

2.4 Contributions of horizontal tail to $C_{m_{cg}}$ and $C_{m_{\alpha}}$

2.4.1 Conventional tail, canard configuration and tailless configuration

2.4.2 Effect of downwash due to wing on angle of attack of tail

2.4.3 Interference effect on dynamic pressure over tail

2.4.4 Expression for $C_{m_{cgt}}$

2.4.5 Estimation of C_{L_t}

2.4. Contributions of horizontal tail to $C_{m_{cg}}$ and $C_{m_{\alpha}}$

In this section the contributions of horizontal tail to $C_{m_{cg}}$ and $C_{m_{\alpha}}$ and the related aspects are dealt with. In this chapter and in chapters 3 and 4, the horizontal tail is simply referred to as tail.

2.4.1 Conventional tail, canard configuration and tailless configuration

A horizontal tail, as explained in this section, provides stability about y- axis. Hence, it is called horizontal stabilizer. When the horizontal stabilizer is behind the wing it is called conventional tail configuration. It is also explained, later in subsection 2.12.3, that for achieving equilibrium with conventional tail configuration, the lift on the tail is generally in the downward direction. This necessitates that the lift produced by the wing has not only to balance the airplane weight but also the negative lift on the tail. This can be avoided if a control surface is located ahead of the wing. Such a configuration is called canard (see Wright flyer in Fig.1.1). It may be added that a canard, being ahead of c.g., has destabilizing contribution to $C_{m_{\alpha}}$. There are airplanes which neither have a horizontal tail nor a canard surface. In this case the airplane is called

“Tailless configuration” (See Concorde in Fig.1.4a). Now, the conventional tail configuration is considered in detail.

The contribution of the tail depends on L_t , D_t and M_{act} (Fig. 2.8). However, these quantities depend on the angle of attack of the tail and the dynamic pressure experienced by the tail. The angle of attack of the tail is not just $(\alpha+i_t)$. The downwash behind the wing affects the angle at which the flow reaches the tail. Further, the wake of the wing and the boundary layer on the fuselage render the dynamic pressure at the tail different from the free stream dynamic pressure. These are called interference effects and are discussed here before describing the contributions of the tail to $C_{m_{cg}}$ and $C_{m_{\alpha}}$.

2.4.2 Effect of downwash due to wing on angle of attack of tail

Wing is the principal contributor to the lift produced by the airplane. While producing the lift, wing induces an angle of attack on the stream around it. The induced angle is positive ahead of the wing and is called upwash. Behind the wing, the induced angle is negative and is called downwash. It may be recalled that in the lifting line theory, used to calculate flow past a finite wing, a bound vortex is located along the quarter chord line and trailing vortices behind the wing. Using this theory the upwash/downwash distribution can be calculated. Typical distribution is shown in Fig.2.12. Its important features are as follows.

- (a) Upwash is zero far ahead of the wing.
- (b) Peak in the upwash occurs slightly ahead of the wing.
- (c) There is downwash at the wing quarter chord and the downwash angle ($\epsilon_{c/4}$) is:

$$\epsilon_{c/4} = (1 + \tau)(C_{LW} / \pi A_w) \quad (2.28)$$

where, C_{LW} is the wing lift coefficient, A_w is the aspect ratio of wing and τ depends on wing parameters like aspect ratio, taper ratio and sweep.

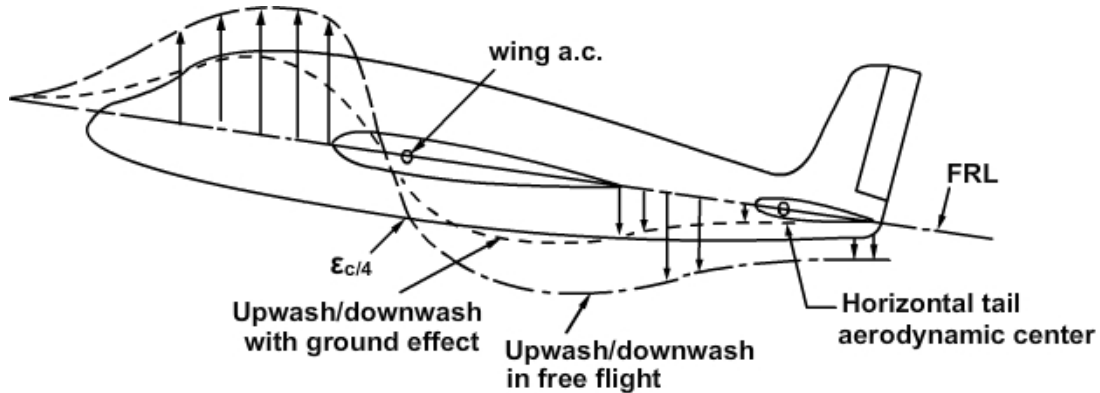


Fig. 2.12 Upwash–downwash field of a wing

(Adapted from Ref.1.12, Chapter 3 with permission from American Institute of Aeronautics and Astronautics, Inc.)

(d) Behind the wing at distances where the tail is located, the downwash angle (ϵ_{fb}) is approximately twice of $\epsilon_{c/4}$.

(e) The upwash/downwash decrease when airplane is near ground as compared to that in free flight.

In a conventional configuration the tail is located behind the wing and would experience downwash i.e. angle of attack of tail would be reduced by ϵ or $\alpha_t = \alpha + i_t - \epsilon$. The value of ϵ would depend on wing parameters, wing lift coefficient, Mach number, tail parameters and location of the tail with respect to the wing.

The common practice is to obtain a value of $d\epsilon/d\alpha$ in subsonic flow based on (a) wing aspect ratio, taper ratio and sweep and (b) location of tail aerodynamic centre with respect to wing and subsequently apply corrections for Mach number effect (see Ref.1.12). Appendix ‘C’ explains the procedure to calculate $d\epsilon/d\alpha$ for a jet airplane.

Remark:

For an elliptic wing the downwash at the aerodynamic centre of the wing ($\epsilon_{c/4}$) is:

$$\epsilon_{c/4} \approx C_{Lw}/\pi A_w \tag{2.29}$$

$$\text{Hence, } \epsilon_{fb} \approx 2\epsilon_{c/4} = 2 C_{Lw}/\pi A_w \tag{2.30}$$

$$\text{Therefore the } (d\epsilon/d\alpha)_{fb} \approx 2C_{L\alpha w}/\pi A_w \tag{2.31}$$

For example if $A_w = 8$, then $C_{L\alpha w} \approx 2\pi \times 8/(8+2) = 5.08/\text{radian}$ and

$$(d\varepsilon/d\alpha)_{fb} = 2 \times 5.08 / (\pi \times 8) = 0.4$$

The tail is generally located far behind the wing and hence the downwash at the tail (ε) is roughly equal to ε_{fb} and Eq.(2.31) can be used to get a rough estimate of $(d\varepsilon/d\alpha)$ even for non-elliptic wings.

2.4.3 Interference effect on dynamic pressure over tail

The dynamic pressure over tail is different from the free stream dynamic pressure due to the following reasons.

(a) Tail may be in the wake of the wing. In a wake the velocity is lowest at the centre and gradually reaches the free stream value (Fig.2.13). The difference between the centre line velocity and the free stream velocity is called velocity defect. The velocity defect depends on the drag coefficient of the wake producing body and the distance behind it. Figure 2.13 shows schematically the wing, the wake centre line and a typical velocity profile of the wake. It is evident that if the tail lies within the wake of the wing, then the dynamic pressure on the tail will be lower than the free stream dynamic pressure.

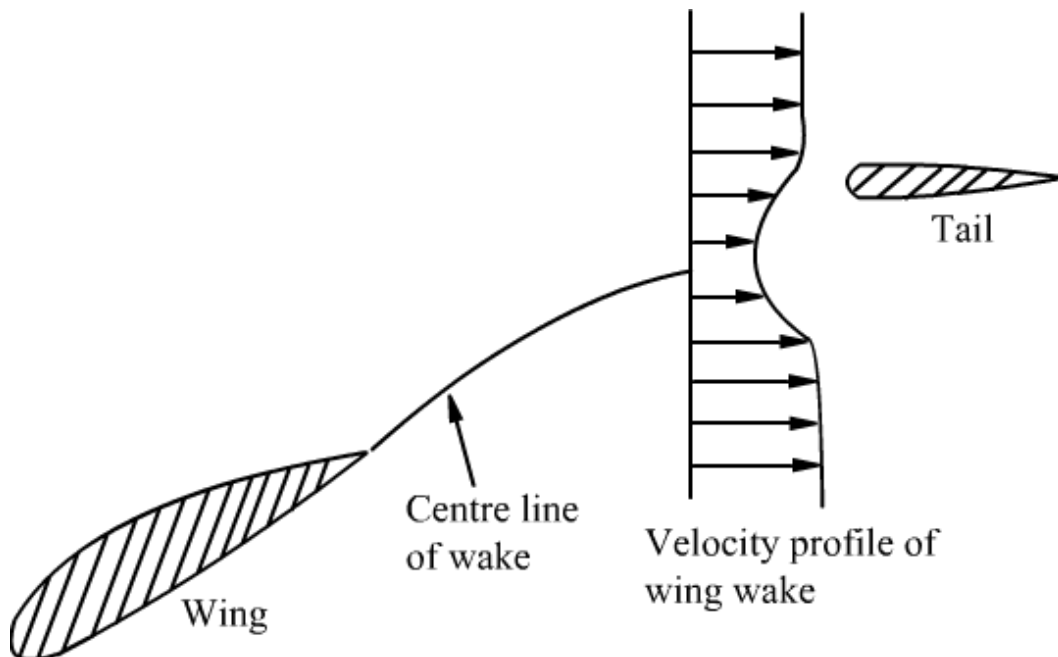


Fig.2.13 Wing, wake centre line and velocity profile of wake - schematic

Flight dynamics –II
Stability and control

(b) Some portion of the tail near its root chord is covered by the boundary layer on the fuselage and as such would experience lower dynamic pressure.

(c) In airplanes with engine propeller combination the slip stream of the propeller may pass over the horizontal tail (Fig. 2.14). It may be recalled that the slip stream of a propeller has higher dynamic pressure than that of the free stream. Hence, the propeller slip stream passing over the tail may increase the dynamic pressure over it in comparison to the free stream dynamic pressure.

The ratio of the dynamic pressure experienced by the tail ($\frac{1}{2} \rho V_t^2$) to the free stream dynamic pressure ($\frac{1}{2} \rho V^2$) is called tail efficiency and denoted by η i.e.

$$\eta = (\frac{1}{2} \rho V_t^2) / (\frac{1}{2} \rho V^2) \quad (2.31a)$$

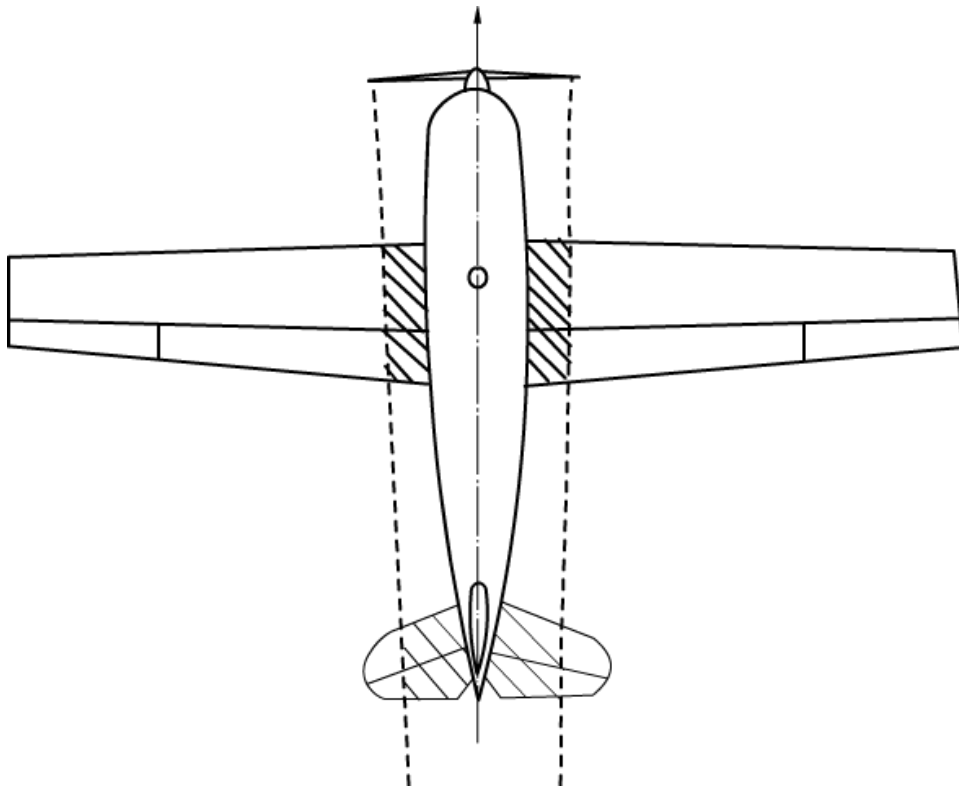


Fig. 2.14 Effect of propeller slip stream on horizontal tail

It is difficult to accurately estimate the value of η . It is assumed between 0.9 and 1.0. It could be more than 1 when the tail is in the slip stream of a propeller.

2.4.4 Expression for C_{mcgt}

With this background the contributions of tail to C_{mcgt} and $C_{m\alpha}$ can now be obtained. Figure 2.15 shows schematically, the forces and moment on the tail.

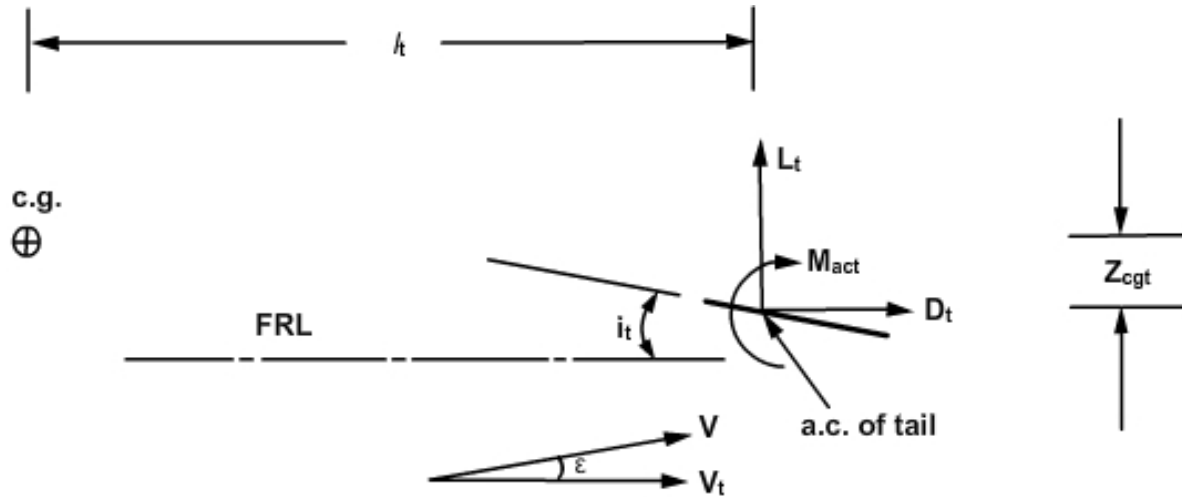


Fig. 2.15 Schematic representation of forces and moment on tail

From Fig.2.15 the angle of attack of the tail is:

$$\alpha_t = \alpha + i_t - \varepsilon = \alpha_w - i_w - \varepsilon + i_t \quad (2.32)$$

Taking moment about c.g.

$$M_{cgt} = -l_t [L_t \cos(\alpha - \varepsilon) - D_t \sin(\alpha - \varepsilon)] + M_{act} - Z_{cgt} [D_t \cos(\alpha - \varepsilon) - L_t \sin(\alpha - \varepsilon)] \quad (2.33)$$

The quantity $(\alpha - \varepsilon)$ is generally small and $\cos(\alpha - \varepsilon)$ is roughly equal to one and terms involving $\sin(\alpha - \varepsilon)$ are ignored. M_{act} is also ignored.

$$\text{Hence, } M_{cgt} = -l_t L_t \quad (2.34)$$

$$= -l_t C_{Lt} \frac{1}{2} \rho V_t^2 S_t \quad (2.35)$$

Consequently,

$$C_{mcgt} = \frac{M_{mcgt}}{\frac{1}{2} \rho V^2 S \bar{c}} = \frac{S_t}{S} \frac{l_t}{\bar{c}} \frac{(1/2) \rho V_t^2}{(1/2) \rho V^2} C_{Lt} \quad (2.36)$$

The term $(S_t/S)(l_t/\bar{c})$ is called tail volume ratio and is denoted by V_H . It may be pointed out that the terms $S_t l_t$ and $\bar{S} \bar{c}$ have dimensions of volume. As

Flight dynamics –II
Stability and control

mentioned earlier, the term $[(1/2)\rho V_t^2]/[(1/2)\rho V^2]$ is called the tail efficiency and denoted by η .

Thus,

$$C_{m_{cgt}} = -V_H \eta C_{L_t}; \quad V_H = \frac{S_t l_t}{S c}; \quad \eta = \frac{\frac{1}{2}\rho V_t^2}{\frac{1}{2}\rho V^2} \quad (2.37)$$

It may be pointed out that typically, $(S_t/S) \sim 0.2$ to 0.25 and $(l_t/c) \sim 2$ to 3 . Hence, V_H lies between 0.4 and 0.7 .

2.4.5 Estimation of C_{L_t}

A tail consists of the fixed portion (stabilizer) and the movable portions namely elevator and tab (Fig.2.16a). The tab is located near the trailing edge of the elevator. Its purpose will be explained in chapter 3. The positive deflections of the elevator (δ_e) and of the tab (δ_t) are shown in Fig.2.16b. A positive δ_e produces increase in C_{L_t} and leads to a negative M_{cg} . The changes in lift coefficient of tail due to α_t , δ_e and δ_t are shown in Fig.2.17.

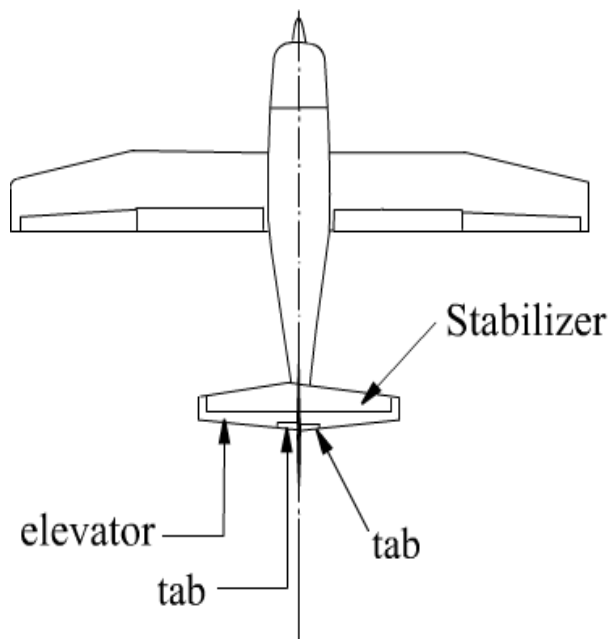


Fig.2.16a Stabilizer, elevator and tab

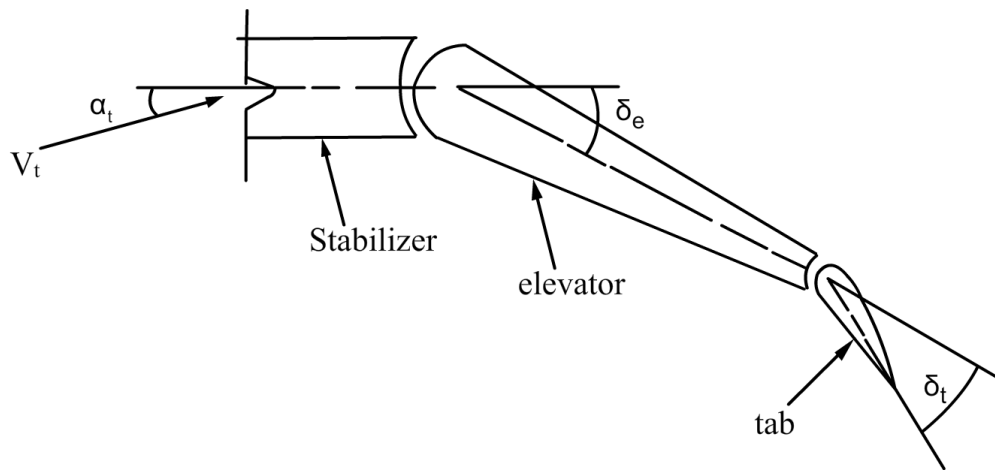


Fig. 2.16b Cross-section of tail with elevator and tab deflected

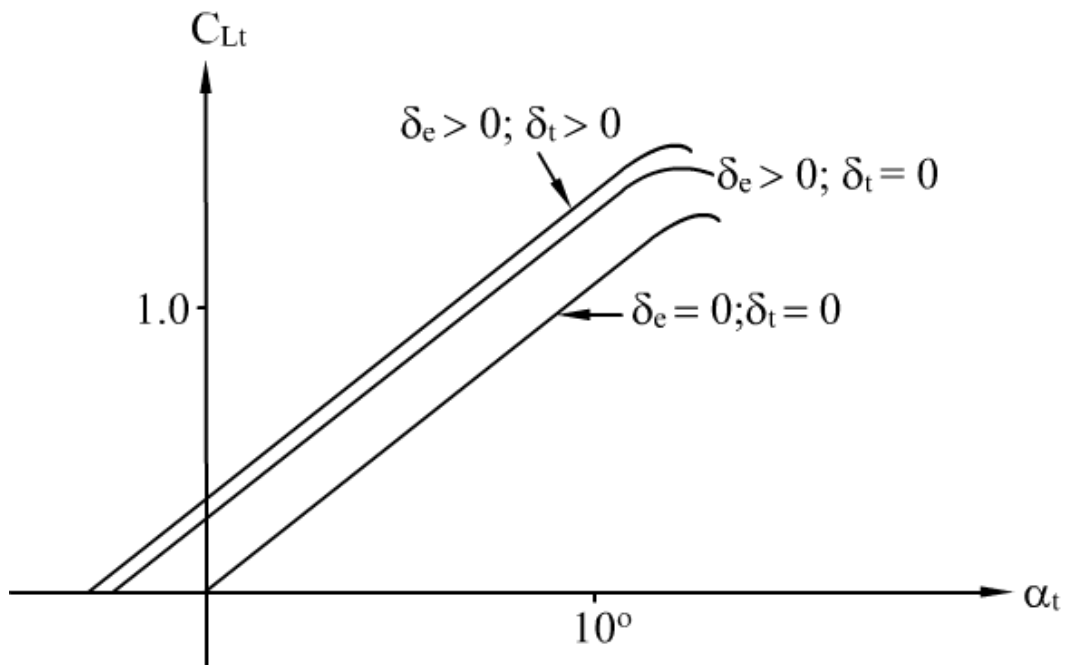


Fig. 2.17 Changes in C_{Lt} due to α_t , δ_e and δ_t

The following may be noted. (a) Generally symmetric airfoils are used on the control surfaces. Hence, C_{Lt} is zero when α_t is zero (b) The elevator is like a flap

Flight dynamics –II
Stability and control

and a downward (or positive) deflection increases C_{Lt} over and above that due to α_t (Fig.2.17). (c) A positive deflection of tab increases C_{Lt} further (Fig.2.17).

(d) Negative deflections of the elevator and tab would have effects opposite of the positive deflections. Taking into account the effects of α_t , $\bar{\delta}_e$ and $\bar{\delta}_t$, the tail lift coefficient can be expressed as:

$$C_{Lt} = C_{Lat} \alpha_t + \frac{\partial C_{Lt}}{\partial \bar{\delta}_e} \bar{\delta}_e + \frac{\partial C_{Lt}}{\partial \bar{\delta}_t} \bar{\delta}_t \quad (2.38)$$

Note: The expression in Eq.(2.38) is valid only when C_{Lt} vs α curve is linear or the angle of attack is below α_{stall} for the tail.

$$\text{Now, } \alpha_t = \alpha - \varepsilon + i_t = \alpha_w - i_w - \varepsilon + i_t \quad (2.39)$$

As noted earlier, ε at a point depends on the wing parameters and location of the point . However, ε is proportional to C_{LW} i.e. $\varepsilon = \text{constant} \times C_{LW}$.

Hence,

$$\varepsilon = \frac{d\varepsilon}{dC_{LW}} C_{LW} = \frac{d\varepsilon}{d\alpha_w} \frac{d\alpha_w}{dC_{LW}} C_{LW} \quad (2.40)$$

$$\text{Further, } \alpha_w = \alpha + i_w \text{ hence, } \frac{d\varepsilon}{d\alpha_w} = \frac{d\varepsilon}{d\alpha}$$

$$\begin{aligned} \text{Consequently, } \varepsilon &= \frac{d\varepsilon}{d\alpha} \frac{1}{C_{L\alpha w}} C_{LW} \\ &= \frac{d\varepsilon}{d\alpha} \frac{1}{C_{L\alpha w}} C_{L\alpha w} (\alpha_w - \alpha_{0LW}) \\ &= \frac{d\varepsilon}{d\alpha} (\alpha + i_w - \alpha_{0LW}) \\ &= \frac{d\varepsilon}{d\alpha} (i_w - \alpha_{0LW}) + \frac{d\varepsilon}{d\alpha} \alpha \\ &= \varepsilon_0 + \frac{d\varepsilon}{d\alpha} \alpha; \quad \varepsilon_0 = \frac{d\varepsilon}{d\alpha} (i_w - \alpha_{0LW}). \end{aligned} \quad (2.41)$$

Remark:

Reference 1.1 uses the following approximate expression:

Flight dynamics –II
Stability and control

$$\varepsilon \approx \frac{2C_{Lw}}{\pi A_w} \quad (2.42)$$

which is the downwash far behind an elliptic wing.

Substituting this, Eq.(2.42) gives:

$$\begin{aligned} \varepsilon &= \frac{2}{\pi A_w} C_{L\alpha w} (\alpha + i_w - \alpha_{0Lw}) \\ \varepsilon &= \frac{2}{\pi A_w} C_{L\alpha w} (i_w - \alpha_{0Lw}) + \frac{2}{\pi A_w} C_{L\alpha w} \alpha \\ \varepsilon &= \varepsilon_0 + \frac{2}{\pi A_w} C_{L\alpha w} \alpha \end{aligned}$$

$$\text{Hence, } \frac{d\varepsilon}{d\alpha} \approx \frac{2C_{L\alpha w}}{\pi A_w} \quad (2.43)$$

As mentioned earlier, $d\varepsilon/d\alpha$ depends on the wing parameters, location of the tail relative to wing and the Mach number.

Noting that $\alpha_w = \frac{C_{Lw}}{C_{L\alpha w}} + \alpha_{0Lw}$, α_t can be written as:

$$\begin{aligned} \alpha_t &= \frac{C_{Lw}}{C_{L\alpha w}} + \alpha_{0Lw} - i_w - \frac{d\varepsilon}{d\alpha} \frac{C_{Lw}}{C_{L\alpha w}} + i_t \\ &= \alpha_{0Lw} - i_w + i_t + \frac{C_{Lw}}{C_{L\alpha w}} \left(1 - \frac{d\varepsilon}{d\alpha}\right) \end{aligned} \quad (2.44)$$

Alternatively, we can write

$$\begin{aligned} \alpha_t &= \alpha - \varepsilon_0 - \frac{d\varepsilon}{d\alpha} \alpha + i_t \\ &= i_t - \varepsilon_0 + \alpha \left(1 - \frac{d\varepsilon}{d\alpha}\right) \end{aligned} \quad (2.45)$$

Putting these together, yields:

$$C_{Lt} = C_{Lat} \left[i_t - \varepsilon_0 + \alpha \left(1 - \frac{d\varepsilon}{d\alpha}\right) \right] + \frac{\partial C_{Lt}}{\partial \delta_e} \delta_e + \frac{\partial C_{Lt}}{\partial \delta_t} \delta_t \quad (2.46)$$